Contribution of Acoustic Emission to Monitor the Effect of Phosphate Based Inhibitor on the Corrosion Behavior of Steel Reinforcement

Haifa NAHALI [1,2], Leila DHOUIBI[2], Hassane IDRISSI [1],

[1] Laboratoire MATEIS CNRS UMR5510 (Équipe CorrIS), INSA-Lyon, F-69621 Villeurbanne, France.
[2] Unité de Recherche « Mécanique-Énergétique », équipe de recherche Corrosion et Protections des Métalliques (COPROMET), ENIT, Université de Tunis El Manar, BP 37 le Belvédère 1002 Tunis, Tunisie.

Abstract. One of the most important causes of reinforced concrete structures deterioration is the corrosion of the reinforcement steel. This corrosion depends on the presence of aggressive agents such as chlorides in the surrounding medium. Numerous protection techniques have been employed to mitigate this corrosion. Among them, the use of corrosion inhibitors has been considered as one of the most effective solutions.

In the present work, the influence of phosphate based inhibitor on the corrosion of reinforcing steels embedded in mortar, and immersed in sodium chloride solution, was investigated by acoustic emission technique. The monitoring of specimens shows that the phosphate based inhibitor addition in the mortar increase the threshold of chloride concentrations, causing the breakdown of steel passivation layer. Thus, the acoustic signatures of concrete fracture and of structure degradation during the corrosion of these specimens have been highlighted. Similarly, the mechanism of phosphate action in terms of preventing steel from corrosion in mortar specimens was analysed by characterization methods (SEM, XRD) of the steel–mortar interface.

Introduction

Steel corrosion in reinforced concrete is one of the main pathologies in civil engineering. Observed predominantly in marine structures and chemical industries, it is also very present in civil and / or nuclear structures: buildings, bridges, seawater pipelines, reactors and nuclear waste containers.The initiation of reinforcing steel corrosion is mainly due to chloride ions in the pore solution of the surrounding concrete, but can only starts once the chloride content at the steel surface has reached a certain threshold value. In literature, this value is generally referred to a critical chloride content or chloride threshold value. This later is expressed according to the ratio R = $[Cl^-]$ / $[OH^-]$ [1]. The knowledge of such values is importance for service life predictions when pitting corrosion is the likely failure

License: http://creativecommons.org/licenses/by/3.0/

mechanism. In service life modelling, chloride threshold values are required as input parameters but to date, no agreement on the reported value is however obtained and it seems to be related to many factors (type of binder, C_3A content, steel concrete interface, ratio of chloride, alkalinity of the pore solution…) [2-6].

Numerous protection techniques have been employed to limit the corrosion risk. Among them, the use of corrosion inhibitors has been considered as one of the most effective solutions. In particular, phosphate-based inhibitors appear promising to protect steel corrosion in concrete, due to their non-toxicity. However, only few authors have investigated this treatment effects in order to elucidate their action mechanism and explain their effectiveness. Previous study [7-10] indicates that inhibitors based phosphate slows chloride ions diffusion and reduces the corrosion rate.

The aim of this work is to evaluate the efficiency of phosphate based inhibitor on the corrosion behavior of reinforcing steels in mortar and immersed in sodium chloride solution. In this context, the acoustic emission technique associated to electrochemical measurements is used to monitor in-situ this phenomena.

1. Experiments

1.1 Materials and concrete mix

The specimens were a reinforced concrete cylinder with a diameter of 30 mm and a length of 60 mm. Reinforcement was a rod (6 mm in diameter and 70 mm long), made of plain carbon steel (C ≤ 0.22) (**Fig. 1**).

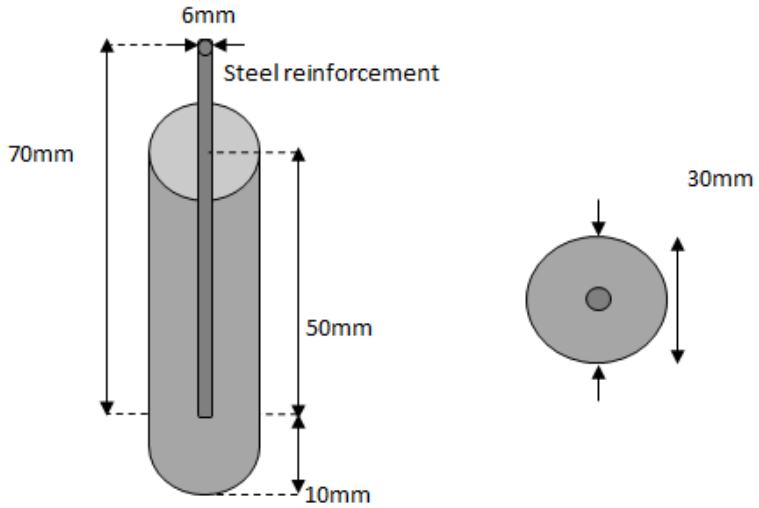

Fig. 1. Test specimen

Before concrete casting, the electrodes are polished using a series of silicon carbide emery papers of grade between 120 and 4000 under a fountain to remove surface defects. The electrode surface area is only along the longitudinal direction, and is equal to 9.42 cm^2. Concrete specimens were made with ordinary Portland and standardized sand. The water cement ratio (w/c) was equal to 0.5 and the cement sand ratio (s/c) to 0.3.

Two types of mortar were prepared; the first one is the reference mortar (blank specimen) such as the mixing water does not contain phosphate inhibitor. For the second

one, the phosphate inhibitor was added to the mortar mixing water, at the content of 0.3 mol per 1Kg of cement. The produced paste is poured into a PVC mold and then compacted using a vibrating table during 60s. The carbon steel reinforcement is placed, afterwards, into the mold according to its longitudinal axis. After casting, all specimens were dried in air for 24h, and then cured in water for 7 days.

After curing days, the upper face of the cylinder is polished with a silicon carbide paper (standard P180) to obtain a smooth surface giving a better contact interface with the acoustic emission sensor.

1.2 Morphology and structure analysis

For SEM observation and EDS analysis, both types of mortars were prepared with the same composition previously described, but using prismatic molds (40 x 40 x 160 mm).These mortars were dried in air for 24h. Then, they were removed from the mold and stored for 28 days in a humid chamber (temperature of 23°C and relative humidity, RH, $\geq$ 95%).

The mortars were split and then small portions of samples were analyzed by Scanning Electron Microscopy (Philips XL20).

1.3 Electrochemical measurements

All tests were carried out in a three-electrode cell with a saturated calomel electrode (SCE) as reference, a platinum electrode as auxiliary and the reinforcement steel in the mortar as working electrode. The corrosion medium of this study is 3% NaCl solution.

In order to accelerate corrosion, anodic potential above the pitting potential (1000mV/SCE) was maintained. Each specimen corresponds to several cycle series of electrochemical measurements as following:

1 - Corrosion potential evolution until stabilization

2 - Polarization curves plot i = f (E)

3 -Anodic polarization at imposed potential (I_{mposed} = 1000mV/SCE) during 12h.

The first series of measurements was carried out, before the anodic polarization (denoted C_0). The second, C_1, is the first series of measurements carried out after the first anodic polarization and C_2 is the second series of measurements recorded after the second anodic polarization etc.

Open circuit potential (OCP) of the specimens were measured during 120 min in immersion in chloride solution. The experimental parameters of potentiodynamic polarization were carried out at a constant scan rate of 25mV/min.

The electrochemical measurements were performed made with a RADIOMETER potentiostat/galvanostat using the VOLTALAB version 3.10 software.

1.4 Acoustic Emission

Acoustic emission was recorded in parallel with the polarization curves. Acoustic emission instrumentation consisted in an acquisition card (MISTRAS), a preamplifier (EPA 1220-gain 60 dB) and a WD piezoelectric sensor (frequency range from 100 to 1000 kHz). The threshold applied for all AE measurements was 28 dB and the sample rate was fixed at 4 MHz with the Mistras software. All recorded signals can be characterized by acoustic parameters as the amplitude; duration...The signals with counts number inferior to three and/or duration inferior to 10 µs were filtered. The acoustic activity is the number of detected AE signals. The energy is the integral of the squared amplitude over time of the

signal duration and is expressed in term of energy units (eu). One eu means 10^{-14} V^2s, corresponding to 10^{-18} J with a reference resistor of 10 kΩ.

2. Results and discussion

2.1 Morphological analysis

After 28 curing days in a humid chamber, mortar samples made up with and without Na_3PO_4 inhibitor were cut and the inner part of each mortar was observed by Scanning Electron Microscope (SEM).

The section observation of the reference mortar shows a high porosity of the mortar (Fig. 2). The energy dispersive analysis (EDS) (Tab. 1) shows the presence of calcium, silicon and aluminum. These elements are characteristic of usual cement hydrate (calcium silicate, aluminates ..).

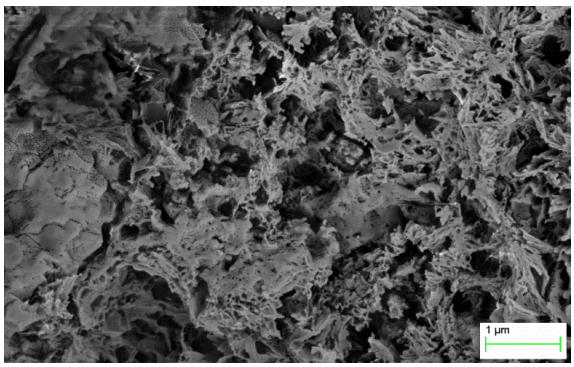

Fig. 2. SEM observation of reference mortar, after 28 days of curing.

Table 1. Composition (Wt. %) determined by EDS analysis of reference mortar, after 28 days of curing.

Elements	O	Al	Ca	Fe	Si
Wt. %	36.9	1.7	42.3	2.5	16.6

The SEM observation of the mortar containing Na_3PO_4 inhibitor (Fig.3) shows the presence of rods dispersed over the entire surface, covering and blocking the most of pores. The EDS analysis (Tab. 2) indicates that these sticks contain essentially phosphorus and calcium elements.

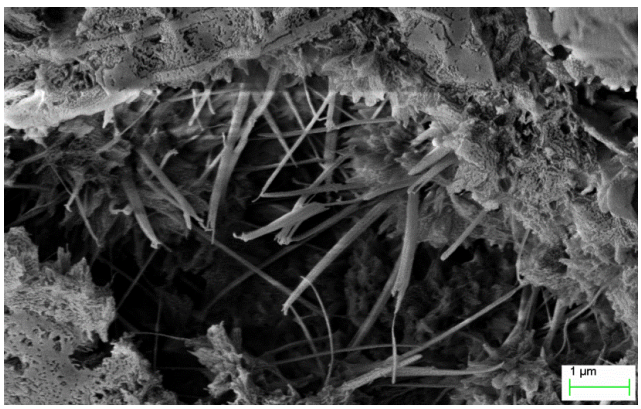

Fig. 3. SEM observation of mortar containing phosphate inhibitor, after 28 days of curing.

Table 2. Composition (Wt. %) determined by EDS analysis of mortar containing phosphate inhibitor, after 28 days of curing.

Elements	O	Al	Ca	Fe	P
Wt. %	22.5	1.7	55.5	1.2	19.2

2.2 Effect of Na_3PO_4 inhibitor on the corrosion behavior of the mortar reinforcement

2.2.1 Polarization curves

The cyclic polarization curves for reinforcing steels in mortar specimens respectively without and with phosphate inhibitor are recorded after 2 hours of immersion in the chloride sodium solution and during each cycle.

The cyclic polarization curves recorded during the first cycle measurement (C_0) for both types of samples are all typical of a system in a passive state (Fig. 4). Indeed, they are characterized by a passivation plateau, a low anodic current density and an absence of hysteresis loop. This behavior indicates that before steel polarization, the passive layer previously formed on the steel surface prevents the corrosion initiation.

For the second cycle (C_1) of the reference specimen tested, polarization curve shows the absence of passivation plateau and the high corrosion current density characterize generalized corrosion, which is typical of an active state. It seems that chloride content, which reaches the reinforcement surface, has greatly exceeded the critical value of steel depassivation. This leads to the corrosion propagation [13-15].

It is only beyond the second anodic polarization (E_{imp}, C_2 cycle) that the electrochemical behavior of phosphate adjuvant system is typical of an active system. The corrosion current density reaches 4.8µA/cm². Chloride ions dissolved in the pore solution, diffuse toward the reinforcement surface and then cause general depassivation. In this case, the phosphate content becomes insufficient to protect the steel from corrosion.

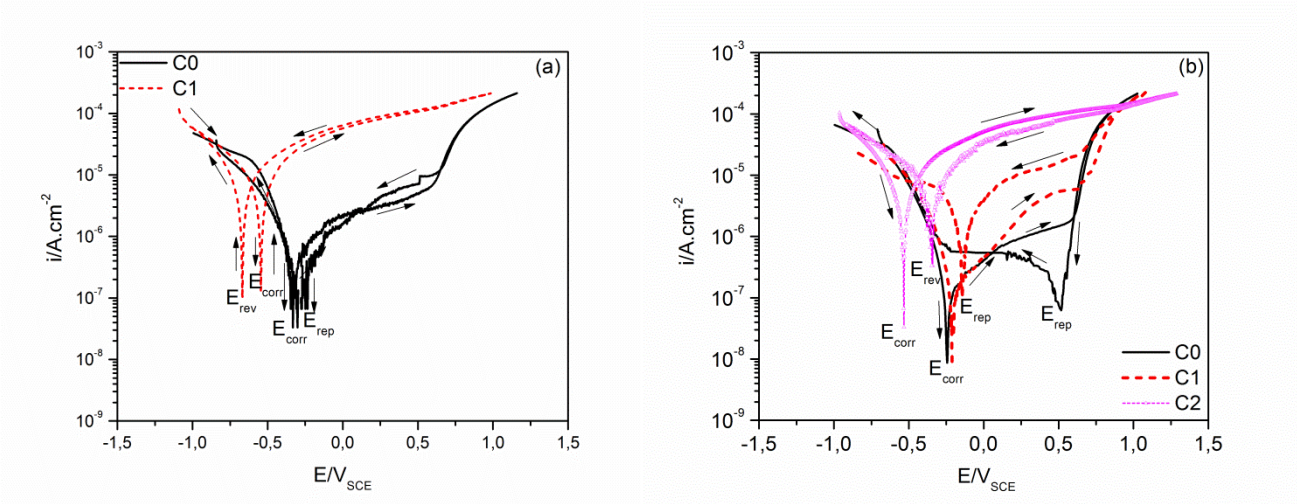

Fig. 4. Cyclic polarization curves for reinforcing steels in mortar specimens without (a) and with phosphate inhibitor (b), recorded during each measurement cycle.

2.2.2 Acoustic emission measurements

The acoustic emission has been recorded in parallel with the polarization curves. During the first polarization curve of the reinforcement (C_0 cycle), almost no acoustic activity has been detected for both types of samples. During the second polarization curve (E_{imp}, C_1 cycle), the acoustic activity is only detected with the reference mortar. This is after the second

anodic polarization (E_{imp}, C_2 cycle), that the acoustic activity occurs for the mortar containing Na_3PO_4. These results are in agreement with those obtained by the electrochemical tests.

Figure 5a and b show the acoustic activity evolution recorded respectively during the C_1 cycle for the reference mortar, and the C_2 cycle for the mortar mixed with Na_3PO_4. A high acoustic activity was observed and various types of signals have been detected. The evolution of the acoustic activity can be characterized by three stages.

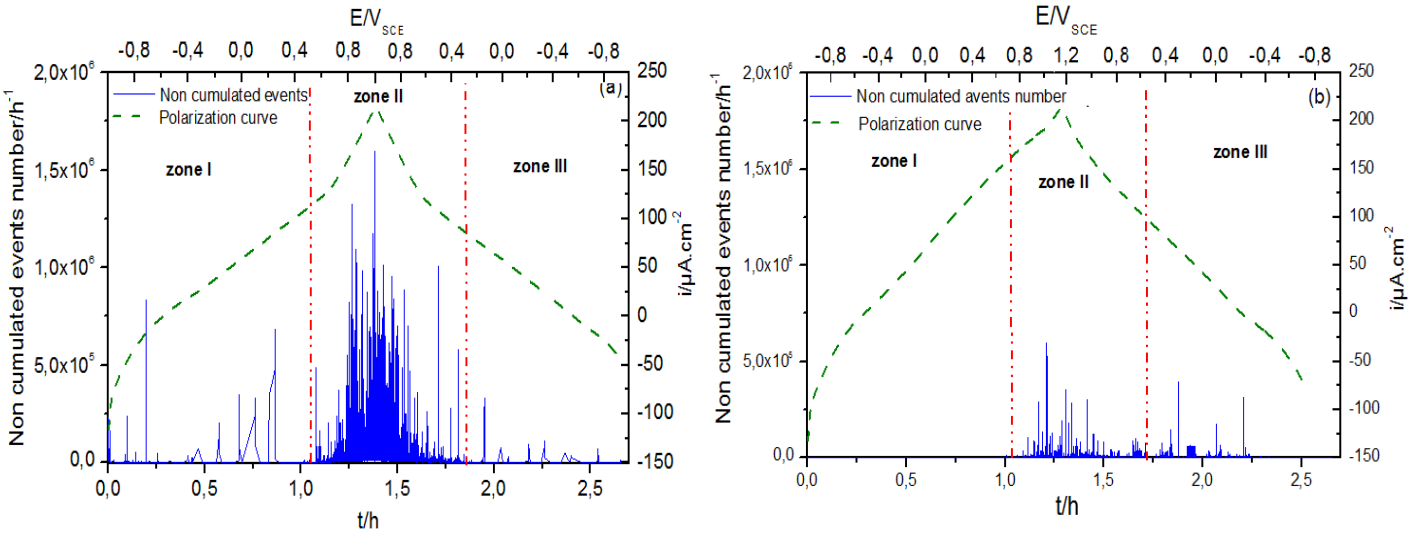

Fig. 5. Polarization curves and acoustic activity correlation for reinforcing steels in mortar specimens without (a) and with phosphate inhibitor (b) recorded in the last cycle of each specimen.

During the first stage (zone I), the current density progressively increases and the acoustic activity is very low. This first period corresponds to the competition between the passivation and depassivation of steel surface by local destruction of the passive layer previously formed on the steel surface. Indeed, the depassivation of the metal are not enough energetic to generate significant acoustic activity [11]. During this stage the signals energy is particularly low (E < 9 e.u) (Fig. 6).

During the second stage (zone II), a significant increase of acoustic activity was observed, due to corrosion propagation. This phenomenon is correlated to the cyclic polarization curve of the reinforcement, which shows an increase of the anodic current density (Fig. 5). The diffusion of a high concentration of chloride ions into the in the mortar leads to the destruction passive layer which causes an attack of the metal and the formation of corrosion products on the surface sample. The presence of these massive corrosion products applies a pressure on the mortar which causes its cracking and subsequently its rupture. These phenomena are responsible for the largest increase of acoustic activity. During this stage, the signals energy is much higher (up to 80 eu) than previously (Fig. 6). Several studies have shown that the propagation of corrosion and crack initiation are characterized by a sudden increase of acoustic activity [16, 17].

The acoustic emission signals recorded during this stage (zone II) are much more energetic than those recorded for the zone I. Two types of signals can be distinguished:

- Signals peak frequency of about 130 KHz, characteristic to the formation of corrosion products and bubbles gas release such as H_2 [18].

- Signals frequency peak from 160 to 200 kHz, is characteristic of micro-cracks propagation [18].

Zone III is characterized by a decrease of the current density and a slight increase of acoustic activity.

On the other hand, the acoustic activity evolution and the signals energy observed in the case of mortar mixed by Na_3PO_4 inhibitor are significantly lower than that obtained with the mortar without inhibitor. The comparison of these results for the mortar with or without inhibitor demonstrates the protective behavior of the Na_3PO_4 inhibitor which decreases the corrosion rate and thus limits the mortar rupture. Indeed, phosphates slowed the chloride diffusion in the mortar and blocks the anodic sites by $FePO_4$ and $Fe_3(PO_4)_2$ precipitation when the armature corrosion is initiated [19].

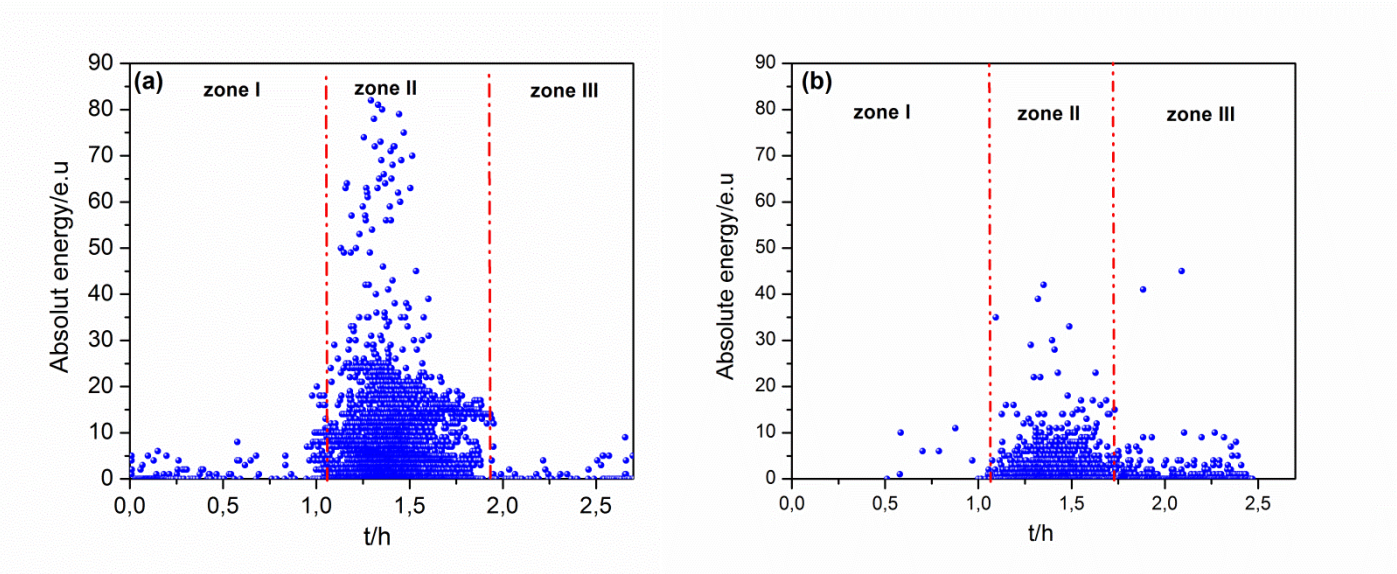

Fig. 6. Absolute energy for reinforcing steels in mortar specimens without (a) and with phosphate inhibitor (b) recorded in the last cycle recorded in the last cycle of each specimen.

Conclusion

The influence of a phosphate based inhibitor on the corrosion behavior of steel reinforcement in mortar immersed in 3%NaCl solution was investigated by electrochemical measurements associated with acoustic emission technique, and completed by SEM observations and EDS analysis. It appears that as, the phosphate content in the vicinity of the reinforcement is high; the passive layer formed on the metal surface protects efficiently the steel against localized corrosion. Indeed, the presence of this inhibitor in the concrete pore solution restrains chloride diffusion to the reinforcement and blocks the anodic sites of reinforcement by forming a stable compounds containing phosphates ($FePO_4$, Fe_3 $(PO_4)_2$). The concentration of Cl^- ions causing the initiation of reinforcement localized corrosion of the reinforcement increases compared to that usually considered in the literature ($0.6.10^{-2}$ mol / L). The correlation between acoustic activity and the polarization curves shows that the AE can be an effective tool for monitoring the degradation of mortar reinforcement.

Acknowledgements

The authors would like to acknowledge the financial support provided by Rhône-Alpes region and the Ministry of Higher Education and Research of France and Tunisia.

References

[1] Verar R, villarroel M, Carvajal A M, Vera E, Ortiz C. Corrosion products of reinforcement in concrete in marine and industrial environments. Mater Chemi and Phys 2009; 114:467-474.

[2] Glass G.K, Reddy B, Buenfeld N.R. The participation of bound chloride in passive film breakdown on steel in concrete. Corros Scien 2000;42: 2013–2021.
[3] Reddy B, Glass G.K, Lim P.J. Buenfeld N.R. On the corrosion risk presented by chloride bound in concrete. Cem & Concr Comp 2002;24: 1–5.
[4] Castel A, Vidal T. François R, Arliguie G. Influence of steel–concrete interface quality on reinforcement corrosion induced by chlorides Magazi of Concr Resear 2003;55: 151–159.
[5] Ann K Y, Song H W. Chloride threshold level for corrosion of steel in concrete. Corros Scien 2007;49: 4113–4133
[6] Ann K Y, Ahn J H, Ryou J S. The importance of chloride content at the concrete surface in assessing the time to corrosion of steel in concrete structures. Construc and Build Mater. 2009;1:239-245.
[7] T.CHAUSSADENT, V.NOBEL, F.FARCAS, I.MABILLE, C.FIAUD, «Effectiveness condiyions of sodium monofluorophosphate as a corrosion inhibitor of concrete reinforcements», Cement and Concrete Research, Vol. 36, (2006), pp. 556-561.
[8] Dhouibi. L, Triki. E, Raharinaivo. A, Trabanelli. G, Zucchi. F. Electrochemical mrthods for evaluating inhibitors of steel corrosion in concrete. British Corrosion Journal 35, 2000, 145-149.
[9] Andrade. C, Alonso. C, acha. M, Malric. B. Preliminary testing of Na_2PO_3F as a curative inhibitor for steel reinforcements in concrete. Cement and Concrete Research; 1992; 22:869-881.
[10] Jiusu Li, Wenbo Zhang, Yong Cao. Laboratory evaluation of magnesium phosphate cement paste and mortar for rapid repair of cement concrete pavement. Construction and Building Materials 2014; 58: 122-128.
[11] Idrissi. H, Limam. A Study and characterization by acoustic emission and electrochemical measurements of concrete deterioration caused by reinforcement steel corrosion. NDT&E International 2003;36: 563–569.
[12] Assouli. B, Simescu. F, Debicki. G, Idrissi. H. Detection and identification of concrete cracking during corrosion of reinforced concrete by acoustic emission coupled to the electrochemical techniques. NDT&E International 2005;38: 682–689.
[13] Hussain. S.E, Rasheeduzafar. S, Al-Musallam. A, Al-Gahtani. A.S. Factors affecting threshold chloride for reinforcement corrosion in concrete. Cemen and Concr Resear 1995;25: 1543-1555.
[14] Saremi. M, Mahallati. E. A study on chloride-induced depassivation of mild steel in simulated concrete pore solution. Cem and Concr Resear 2002;32: 1915-1921.
[15] Ming-Te. L, Ji-Jie. L. Reliability analysis for the existing reinforced concrete pile corrosion of bridge substructure. Cem and Concr Resear 2005; 35: 540-550.
[16] Shaikh. H, Amirthalingam. R, Anita. T, Sivaibharasi. N, Jaykumar. T, Manohar. P, Khatak. HS. Evaluation of stress corrosion cracking phenomenon in an AISI type 316 L stainless steel using acoustic emission technique. Corros Scien 2007; 49:740-765.
[17] Kovač.J, Leban. M, Legat. A. Detection of SCC on prestressing steel wire by the simultaneous use of electrochemical noise and acoustic emission measurements. Electroch Acta 2007;52: 7607-7616.
[18] Ramadan. S, Gaillet. L, Tessier. C, Idrissi H. Detection of stress corrosion cracking of high-strength steel used in prestressed concrete structures by acoustic emission technique. Appl Surf Scien 2008;254: 2255–2261.
[19] Nahali. H, Dhouibi. L, Idrissi. H. Effect of phosphate based inhibitor on the threshold chloride to initiate steel corrosion in saturated hydroxide solution. Construc and Build Mater 2014;52: 87-94.